CHEMISTRY
AN ASIAN JOURNAL
www.chemasianj.org

Accepted Article

Title: The “nitrogen effect”: Complexation with macrocycles potentiates fused heterocycles to form halogen bonds in competitive solvents

Authors: Kwaku Twum, Sanaz Nadimi, Frank Boateng Osei, Rakesh Puttreddy, Yvonne Bessem Ojong, John J. Hayward, Kari Rissanen, John F. Trant, and Ngong Kodiah Beyeh

To be cited as: *Chem. Asian J.* **2023**, e202201308

Link to VoR: https://doi.org/10.1002/asia.202201308

A Journal of
ACES Asian Chemical Editorial Society

A sister journal of **Angewandte Chemie** and **Chemistry – A European Journal**

WILEY-VCH

10.1002/asia.202201308

WILEY-VCH

RESEARCH ARTICLE

The "nitrogen effect": Complexation with macrocycles potentiates fused heterocycles to form halogen bonds in competitive solvents

Kwaku Twum,[a] Sanaz Nadimi,[b] Frank Boateng Osei,[a] Rakesh Puttreddy,[c] Yvonne Bessem Ojong,[a] John J. Hayward, [b] Kari Rissanen,[c] John F. Trant, [b] and Ngong Kodiah Beyeh*[a]

[a] Dr. K. Twum, F.B. Osei, Dr. Y.B. Ojong, Prof. N.K. Beyeh*
Department of Chemistry
Oakland University
146 Library Drive, Rochester, Michigan, 48309, USA
beyeh@oakland.edu
[b] S. Nadimi, Dr. J.J. Hayward, Prof. J.F. Trant
Department of Chemistry and Biochemistry,
University of Windsor,
401 Sunset Avenue, Windsor, Ontario, N9B 3P4, Canada
[c] Dr. R. Puttreddy, Prof. K. Rissanen
Department of Chemistry
University of Jyvaskyla
Survontie 9 B, FI-40014 Jyvaskyla, Finland

Supporting information for this article is given via a link at the end of the document.

Weak intermolecular forces are typically very difficult to observe in highly competitive polar protic solvents as they are overwhelmed by the quantity of competing solvent. This is even more challenging for three-component ternary assemblies of pure organic compounds. In this work, we overcome these complications by leveraging the binding of fused aromatic N-heterocycles in an open resorcinarene cavity to template the formation of a three-component halogen-bonded ternary assembly in a protic polar solvent system.

Introduction

Calixarenes, resorcinarenes, and other macrocyclic cavitands are widely studied hosts for many guest systems.[1–4] These hosts are known for their ability to bind molecular guests through multiple non-covalent interactions in their tailored but shallow internal cavities.[5] Amongst many architectures reported, two-component dimeric and hexameric capsules are relatively common[6,7] while all organic three-component assemblies are relatively rare.[8,9] One key advantage of these host compounds is the ease of functionalization on either the upper or lower rim.[10–12] The possibility of functionalizing resorcinarene with fluorescent groups makes them potentially useful point-of-care sensors for diagnostics.[13] However, a major limitation in the application of these macrocycles to solve biomedical challenges is that the choice of guest is restricted to small molecules, with salts preferred for the stronger potential for stable interactions. The utility of the systems would be greatly expanded by taking advantage of the emergent properties of a bound guest that can interact with a third component. We recently reported on a series of ternary complexes whereby a C-$_{ethyl}$-2-methylresorcinarene binds a pyridine in its internal cavity; both components of the resulting complex can then synergistically participate in hydrogen bonds with different carboxylic acids to form tight ternary complexes.[8] The pK_a of the carboxylic acids was critical in determining the robustness of the ternary assemblies; some were very stable in quite competitive solvent environments. Proton transfer was also observed in the ternary assembly of carboxylic acids with very low pK_a values.

Aromatic nitrogen heterocyclic (N-heterocycles) motifs — *e.g.* pyridine, quinoline, and imidazole — are widespread in nature and quite prevalent in biological and pharmaceutical compounds.[14–19] When protonated, they can form host-guest complexes with aromatic cavity-containing macrocycles through cation-π interactions.[14,20,21] Their complexes with artificial receptors such as crown ethers have also been widely reported.[22–24] There are several reports of complexes of resorcinarenes with aromatic nitrogen heterocycles, however, in the majority of these reports, the aromatic N-heterocycles such as pyridine and 4,4′-bipyridine are mostly used as building blocks in the construction of multicomponent architectures. There are also reports of complexes between nucleosides, their derivatives and resorcinarenes.[25] Rissanen and co-workers reported several crystal structures of *endo*-complexes of five aromatic N-heterocycles with C-$_{ethyl}$-resorcinarenes highlighting π-π and C–H···π to be the key interactions.[20]

Halogen bonding (XB) is a highly directional non-covalent interaction occurring between electron-deficient halogen atoms and a Lewis base.[26,27] This affinity results from an electropositive region on a halogen atom that is polarized by electron-withdrawing groups.[28,29] Due to the high polarizability of the larger halogen atoms, the strength of the XB increases as radius increases: I > Br >> Cl >>> F; the more electropositive halogens yield stronger interactions. While polarized electrostatic attractions are critical to halogen binding, it is in effect a composite of charge transfer, van der Waal's interactions, and dipole-dipole interactions.[30] Aromatic N-heterocycles such as pyridine are potent XB acceptors. Rebek and coworkers reported amplified XB between an N-containing pyridine and O-containing δ-lactone with iodoperfluorinated propane and butane inside a sealed hydrogen bonded dimeric deep cavity cavitand capsule in a non-competing, non-polar, 1,3,5- trimethylbenzene-d^{12} solvent.[31] The nature of the solvent is essential: non-polar solvents can drive the mutual interaction of polar components, stabilizing any complex. Furthermore, in their report, the guest and the XB donor were all trapped inside a sealed dimeric capsule, greatly increasing local concentration, so the components were forced to interact. We wished to see if we can similarly leverage the electron-rich internal cavity of resorcinarenes as hosts for fused aromatic N-heterocycles in a potential 3-component open assembly. Herein, we aim to investigate the following: a) can we harness the preference for N-heterocycles as suitable guest of *endo*-complexation with resorcinarenes? Will these *endo*-complexations lead to open inclusion complexes or capsular assemblies? b) If open inclusion complexes, can the fused aromatic N-heterocycle, when anchored in the cavity of the resorcinarene, participate in halogen bonding as an XB acceptor in a three-component ternary assembly in a competitive solvent environment?

10.1002/asia.202201308
WILEY-VCH

RESEARCH ARTICLE

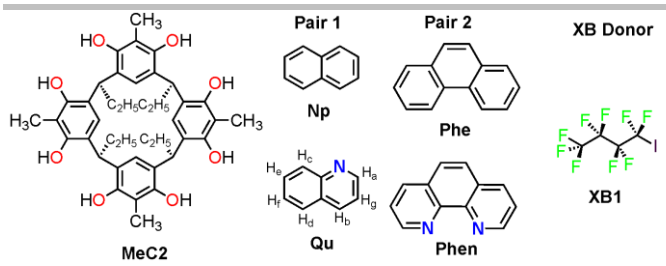

Figure 1. Structures of C_{ethyl}-2-methylresorcinarene (**MeC2**) as host, fused aromatic naphthalene and phenanthrene (**Np**, **Phe**), fused aromatic N-heterocycle quinoline and phenanthroline (**Qu**, **Phen**) as guests and XB acceptor, and 1-iodononafluorobutane (**XB1**) as XB donor.

To answer these questions, we selected a C_{ethyl}-2-methylresorcinarene (**MeC2**) as host, fused aromatic naphthalene and phenanthrene (**Np**, **Phe**), fused aromatic N-heterocycle quinoline and phenanthroline (**Qu**, **Phen**) as guests and XB acceptor, and 1-iodononafluorobutane (**XB1**) as XB donor (Figure 1)

Results and Discussion

Complexation studies in pure methanol

Studying solution-phase host-guest complexation of a macrocycle using NMR spectroscopy is well established.[32–34] In our case, very limited changes were observed in chloroform between the isolated components and physical mixtures, and so we selected methanol as a solvent. In methanol, the complexes are in rapid equilibrium with the free components, therefore only one peak is observed in their NMR spectra as an average of the free and complexed species. Lower ppm values (shielding) of a guest's proton signals are characteristic of a guest predominantly in the cavity of the macrocycle. Moreover, the orientation of the guest within the cavity can be deduced by comparing the degree of shielding of the guest protons; the effect is greater for those deeper in the resorcinarene cavity.[8,31,35] In addition, the degree of shielding can also be used as a qualitative indication of the strength of association between the host and guests.[36–39] In this study, we also use ^{1}H NMR to highlight the difference in host-guest complexation between the pairs of guests **Np** and **Qu**, and **Phe** and **Phen** to explore the "nitrogen effect". For example, significant shielding of **Qu**'s proton signals compared to those of **Np** suggests **Qu** and the host predominantly exist as binary *endo*-complexes in solution. Furthermore, the greater degree of shielding for ^1H_b and ^1H_g compared to ^1H_a and ^1H_c shows the guest sits in the hydrophobic cavity in a way that orients the *N* atom to the solvent environment (Figure 2). This binary complex affords two unique properties compared to free quinoline in solution that can be leveraged for a stronger halogen bond: 1) the host's hydrophobic cavity restricts free molecular rotation of bound **Qu**, and 2) the orientation of the Lewis basic *N* atom towards the solvent orients and accommodates the directionality of a halogen bond in solution. Similarly, significant shielding of the fused N-heterocycle **Phen** signals were observed with very limited shift changes to the resonances in the fused **Phe** compound (Figure S2).

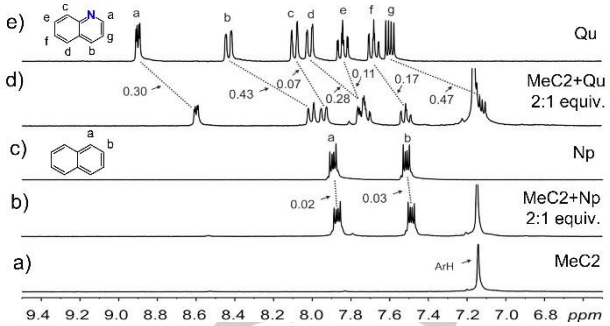

Figure 2. An expansion of the ^{1}H NMR (CD_3OD, 298 K, 300 MHz) of **MeC2** complexes with **Np** and **Qu**. Spectra are produced from (a) 20 mM **MeC2**, (c) 20 mM **Np**, (e) 20 mM **Qu**, 2:1 mixture of (b) **MeC2** (40mM) and **Np** (20mM), and 2:1 mixture of (d) **MeC2** (40mM) and **Qu** (20mM). Dashed lines highlight the observed shift changes of the resonances, labels are in ppm.

Resorcinarenes form capsular assemblies in solution.[40–46] Our group and others have reported dimeric capsular assemblies of unfunctionalized resorcinarenes in methanol with suitable guests such as ammonium or phosphonium cations.[47–50] To determine if these N-heterocycles template capsular assemblies in methanol solution, we turned to 2D diffusion ordered NMR spectroscopy (DOSY). DOSY is a suitable technique to determine intermolecular interactions in solution because the diffusion coefficient of a molecular species under specific conditions (*e.g.* concentration, solvent, temperature etc) depends on its molecular weight, size, and shape. First, we used 2D DOSY to measure the diffusion coefficient of the guests (**Qu** and **Phen**), and **MeC2** in pure methanol (Table 1). The diffusion coefficients ($D \times 10^{-9}$ in m^2s^{-1}) of **MeC2**, **Qu**, and **Phen** were calculated in the self-assembly of host-guest solutions. Larger molecules have smaller diffusion coefficients compared to small molecules. From the DOSY results, we determined that **MeC2** forms open 1:1 inclusion complexes with **Qu** (Table 1) which makes the **Qu** available to engage with a third species via halogen bonding. No reliable diffusion coefficient was observed for **Np** which is likely due to its very weak interactions with **MeC2**. Interestingly, **MeC2** forms a 2:1 dimeric capsular assembly with the N-heterocycle **Phen** in pure methanol and an open 1:1 inclusion complex with the fused aromatic **Phe** (Table 1, Figure 3, Figure S7).

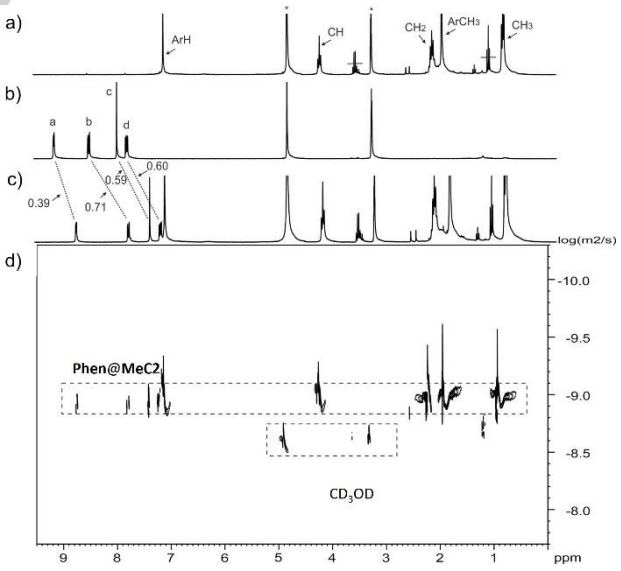

Figure 3. The ^{1}H NMR (CD_3OD, 298 K, 300 MHz) of **MeC2** complex with **Phen**. Spectra are produced from (a) 20 mM **MeC2**, (b) 20 mM **Phen**, (c) 2:1 mixture of **MeC2** (40 mM) and **Phen** (20 mM), (d) 2D DOSY NMR spectra (CD_3OD, 298 K, 300 MHz) of a 2:1 mixture of **MeC2:Phen**, showing the chemical species present in the sample. Chemical shifts [ppm] are shown on the x-axis and the diffusion coefficients [log m^2s^{-1}] on the y-axis of the 2D plot. Dashed lines

10.1002/asia.202201308

highlight the observed shift changes of the resonances, labels are in ppm. Star represent the residual solvent.

Table 1. Average Diffusion Coefficients D ($\times 10^{-9}$ m^2s^{-1}) of the host, the guests, and the host-guest mixtures at 298 K.

Sample in CD_3OD[a]	D, Guest	D, Host
MeC2	-	1.020±0.110
Np	2.490±0.200	-
Qu	2.260±0.070	-
Phe	2.440±0.010	-
Phen	1.360±0.040	-
MeC2 + Np (2:1)	-[c]	1.190± 0.210
MeC2 + Qu (2:1)	1.930±0.350	1.010±0.240
MeC2 + Phe (2:1)	2.020±0.230	1.050±0.200
MeC2 + Phen (2:1)	0.950±0.010	0.820±0.010
Samples in 50/50 CD_3Cl: CD_3OD[b]		
MeC2	-	0.569±0.040
Qu	1.520±0.118	-
MeC2 + Qu	1.331± 0.027	0.489±0.004
MeC2 + Qu + XB1 (1:1:1)	1.325± 0.021	0.490±0.002
Phen	1.148±0.090	
MeC2 + Phen (1:1)	1.049±0.001	0.489±0.008
MeC2 + Phen + XB1 (1:1:2)	1.036±0.001	0.479±0.009

[a,b]Diffusion coefficients of CD_3OD ranges between 1.840–2.090$\times 10^{-9}$ m^2s^{-1}. [c]Poor relaxation. No reliable diffusion coefficient for **Np** probably because of a relatively weak binding process.

X-Ray crystallography

Although the nature of a species in the solid state may not reflect its interactions in solution, and care must be taken in interpretation, X-ray crystal structures provide unambiguous information about possible interactions. Co-crystallization of **Phen** with **MeC2** in MeOH resulted in a water-mediated dimeric capsule, **Phen**@(**MeC2**)$_2$·9H_2O, consistent with the dimeric capsule in solution observed by DOSY NMR. All attempts at crystallization of the **MeC2** with the other guests from MeOH resulted only in homocrystals of either host or guest molecules. In the capsule **Phen**@(**MeC2**)$_2$, two molecules of **MeC2** are joined together by $_{host}$(H-O)···H_2O···(H-O)$_{host}$ hydrogen bond interactions and take on an eclipsed conformation, which is most likely related to the involvement of the *endo*-guest and water molecules in mediating the capsule. The centroids of the planes, defined by the hosts' methine carbons, are separated by a distance of 11.64 Å, which is longer than the distances reported for dimeric capsules encapsulating tetraalkylammonium salts.[51] This can be attributed to the larger size of the **Phen**. The **Phen** is situated inside the cavity, and the C-H interactions between its C–H groups and the **MeC2** aromatic rings range from 2.71 to 3.0 Å.

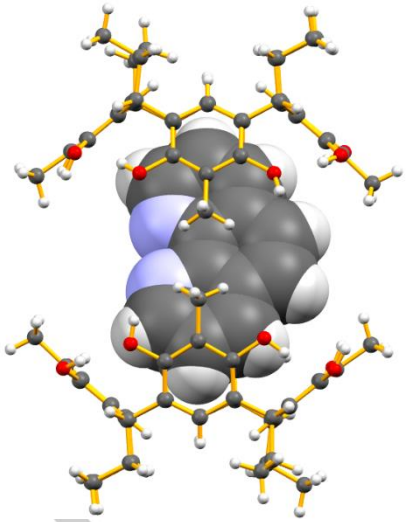

Figure 4. X-ray structure of the host–guest dimeric 2:1 capsule **Phen**@(**MeC$_2$**)$_2$. Ball and stick representation with the guest in CPK mode. Disordered guest and water molecules are not shown for viewing clarity.

Complexation studies in methanol-chloroform mixture

The high dielectric constant makes methanol a highly competitive solvent and thus non-ideal for the formation of halogen bonds in solution. Chloroform is a much better solvent for halogen bonding; however, host-guest complexes were not observed in pure chloroform. In order to investigate the possibility of a halogen bonded ternary assembly, we turned to a 50/50 v/v methanol/chloroform solvent mixture. Even at 50%, methanol is still, of course, strongly able to interfere in the formation of any but the strongest XBs. To obtain an indication of a potential host-guest system that could form XBs, we prepared equimolar mixtures of **MeC2** and either **Qu** or **Phen**. The nitrogen effect is still observed, resulting in shifts to lower ppm of the guest signals, indicating *endo*-complexation in this mixed solvent system (Figure 5). As expected, when comparing these systems to the same ones in pure methanol, the degree of shielding is less pronounced (Figures 2, 5).

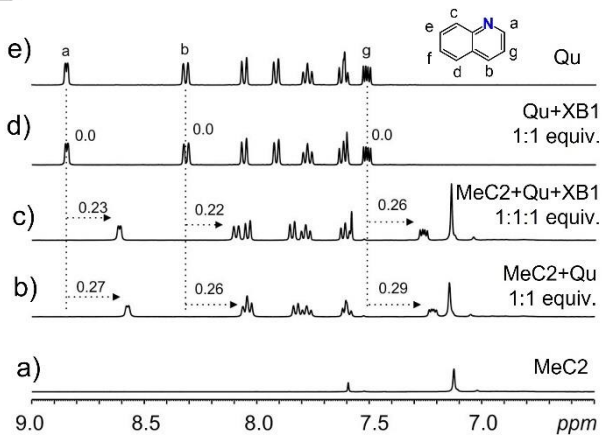

Figure 5. An expansion of the ^{1}H NMR ($CD_3OD/CDCl_3$, v/v, 298 K, 300 MHz) of **MeC$_2$** complexes with **Qu** (20 mM) and **XB1** (20 mM). Spectra are produced from (a) **MeC2**, (e) **Qu**, equimolar mixtures of (b) **MeC2**+**Qu**, (d) **Qu**+**XB1**, and (c) **MeC2**+**Qu**+**XB1** (20 mM each). Dashed lines highlight the observed shift changes of the resonances, labels are in ppm.

XB1 is known to form potent halogen bonds with pyridine and other nitrogen-containing aromatic compounds.[26] However, these studies have been done in non-competing solvents such as pure chloroform. This is because protic and highly polar solvents will provide strong competition as halogen bond acceptors and will inhibit the stability of XBs in solution. To identify halogen

10.1002/asia.202201308

bonding we first monitored the ^{1}H NMR signals of **Qu** for indication of potential halogen bonding in an equimolar mixture with **XB1**. Of particular significance is the H_a closest to the nitrogen acceptor since this is most sensitive to changes in the chemical environment on the nitrogen. No signal changes were observed (Figure 5). The ^{19}F NMR of the fluorine attached to the same carbon as the iodine reveals very small changes of only −0.01 ppm (Figure 6). We then turned to ^{13}C NMR by monitoring the carbon closest to the nitrogen (carbons "a" and "i", Figure 7). Small shifts of 0.15 and 0.14 ppm lower were observed. The ^{1}H, ^{19}F and ^{13}C NMRs all reveal very weak to no XB between **Qu** and **XB1** in this mixed and highly competing methanol-chloroform solvent system. However, we know that **MeC2** forms *endo*-complexes with either **Qu** or **Phen** in this mixed solvent system. We hypothesized that this complex, holding the guest in a defined conformation and increasing the electron density on the guest, might be sufficient to make **Qu** a suitable XB partner for **XB1.** The ternary assembly might be able to do what a binary system cannot accomplish. For example, the halogen bond interaction can be enhanced in the ternary assembly compared to binary system. Consequently, we titrated one equivalent of **XB1** into a 1:1 mixture of **MeC2** and either **Qu** or **Phen**. First, we compared the ^{1}H NMR of the two-component (pre-titration) and three-component mixtures. In the two-component mixture, the **Qu** H_a protons move 0.27 ppm lower, signifying complexation in the hydrophobic cavity. In the same solvent mixture, 1 equivalent of **XB1** causes H_a to be shielded by 0.23 ppm to accommodate the halogen bond while in-cavity. Next, we conducted ^{19}F NMR experiments to monitor the fluorine signals of **XB1** in similar three-component self-assembly. Similarly, we monitored the fluorine signals on the same carbon as the iodine as they are most sensitive to halogen bond formation. For comparison, in a 1:1 mixture of **Qu** and **XB1**, the fluorine signals of interest only moved by −0.01 ppm. In the ternary mixtures, this signal moves by −0.06 ppm (Figure 6). This can be interpreted as an increase in the number of halogen bonded species due to the macrocycle but could also be due to an unintended interaction of the macrocycle. To provide additional evidence, we conducted ^{13}C and 2D DOSY NMR of the **MeC2**, **Qu** and **XB1** in the mixed solvent system (Table 1).

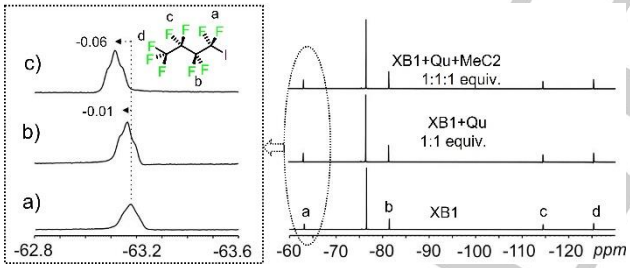

Figure 6. An expansion of the ^{19}F NMR ($CD_3OD/CDCl_3$, v/v, 298 K, 300 MHz) of **XB** complexes with **Qu** and **MeC2**. Spectra are produced from (a) **XB1** (20 mM) and equimolar mixtures (20 mM) of (b) **MeC2**+**Qu**, (d) **Qu**+**XB1**, and (c) **MeC2**+**Qu**+**XB1**. Dashed lines highlight the observed shift changes of the resonances, labels are in ppm.

The ^{13}C NMR of the ternary mixture shows a significant shift in the resonances compared to any of the binary systems (**MeC2**+**Qu** and **Qu**+**XB1**). Taking carbon "a", closest to the nitrogen of **Qu**, the ternary mixtures show a lower ppm shift of 1.03 with only 0.50 ppm for **MeC2**+**Qu** and 0.15 ppm for **Qu**+**XB1** mixtures. Even bigger shift changes are observed for carbon "i": 1.44 ppm in the ternary mixture as compared to 0.47 ppm and 0.14 ppm for the **MeC2**+**Qu** and **Qu**+**XB1** mixtures respectively (Figure 7). These results thus support the presence of a ternary system held together by XB and C−H···π interactions as well as size complementarity.

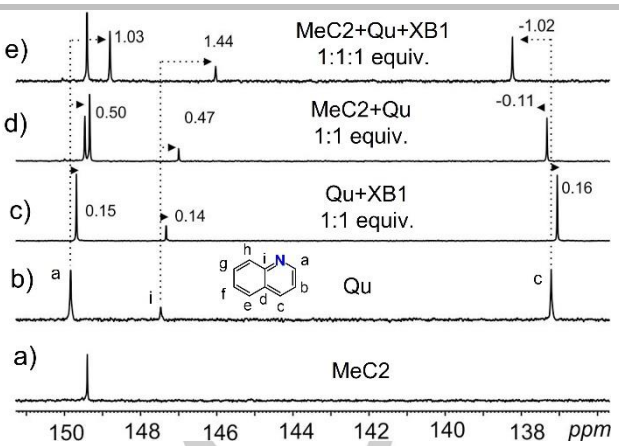

Figure 7. An expansion of the ^{13}C NMR ($CD_3OD/CDCl_3$, v/v, 298 K, 400 MHz) of **MeC$_2$** complexes with **Qu** (20 mM) and **XB1** (20 mM). Spectra are produced from (a) **MeC$_2$**, (b) **Qu**, equimolar mixture of (c) **Qu**+**XB1** (20 mM each), (d) **MeC2**+**Qu** (20 mM each), and (e) **MeC2**+**Qu**+**XB1** (20 mM each). Dashed lines highlight the observed shift changes of the resonances, labels are in ppm.

To get further insights into these assemblies in the mixed solvent systems, we used 2D DOSY NMR. Unfortunately, the diffusion coefficients of **XB1** cannot be measured directly due to the absence of hydrogen atoms. Looking at the different mixtures of **MeC2**, **Qu** and **XB1** as an example, the results show diffusion coefficients of $0.569\pm0.040\times10^{-9}$ m^2s^{-1} and $1.520\pm0.118\times10^{-9}$ m^2s^{-1} for the pure **MeC2** and **Qu** respectively. The binary mixture reveals diffusion coefficients of $0.489\pm0.004\times10^{-9}$ m^2s^{-1} and $1.331\pm0.027\times10^{-9}$ m^2s^{-1} for **MeC2** and **Qu** respectively. In the three-component mixture, diffusion coefficients $0.490\pm0.002\times10^{-9}$ m^2s^{-1} and $1.325\pm0.021\times10^{-9}$ m^2s^{-1} for **MeC2** and **Qu** respectively. The diffusion coefficients give $0.489\pm0.008\times10^{-9}$ m^2s^{-1} and $1.049\pm0.001\times10^{-9}$ m^2s^{-1} as well as $0.479\pm0.009\times10^{-9}$ m^2s^{-1} and $1.036\pm0.001\times10^{-9}$ m^2s^{-1} for **MeC2** and **Qu** in the binary and ternary mixtures respectively. In a capsular construct, the diffusion coefficients should be the same as all components move together. However, in an open inclusion complex, we expect a dynamic equilibrium between the complex and the monomeric species, and as the monomeric species are different sizes, and as the on-off rates are fast, we get a single value for each species where decreases in the diffusion constants suggest interaction. In these two components and three-component mixtures, the decrease in the diffusion coefficients of both **MeC2** and **Qu** and **Phen** show they all are more likely to participate in a larger assembly in both the binary and ternary mixtures.

Quantification of binding

Lastly, we employed isothermal titration calorimetry (ITC) to quantify some of the binding processes and get an insight into the thermodynamics of the binding. The thermodynamics of host-guest complexation were assessed using a series of ITC experiments in 50:50 methanol and chloroform (Figure S15-17, Table 2). The parameters K_a, ΔH, ΔS, and ΔG were determined by fitting the ITC curves to a one-site binding model. Given the competitive nature of the solvent environment for XB formation, the thermodynamics of the ternary system formation cannot be reliably determined without large errors. The effect of the nitrogen on the fused aromatic is also observed in the self-assembly of the guests with the host **MeC2**. Complex formation between **MeC2** and the **Qu** was spontaneous ($\Delta G<0$) at 298 K. This self-assembly is enforced by the methanol that drops the hydrophobicity of the solvent to favor *endo*-complexation in the cavity of the resorcinarene. The negative ΔH and positive $T\Delta S$ values indicate the complexation is favored by both enthalpy and entropy. However, this self-assembly does not occur between **MeC2** and **Np** (Figure S15). Moreover, the ITC titration of the **Qu** with **XB1** establishes the halogen bond formation between the two components in the mixed solvent system. It is noteworthy that the

strength and directionality of the halogen bond is dependent on the magnitude and size of the sigma hole.[52] The association constant between **Qu** and **XB1** was measured at 345±28.4 mol^{-1}. The complexation is enthalpically favorable, releasing heat to the solvent environment. However, entropy contributions in the halogen bonding with **XB1** require a low reaction temperature to maintain spontaneous self-assembly.

Table 2. Thermodynamic binding parameters of formed complexes between the host (10 mM) and the guests (50 mM) by ITC[a]

Complex	K_a	ΔH kcal/mol	$T\Delta S$ kcal/mol	ΔG kcal/mol
Qu@MeC2	699±122	−0.96±0.085	2.92	−3.88
Np@MeC2	-[a]	-[a]	-[a]	-[a]
Qu@XB1	345±28.4	−5.02±0.092	−1.56	−3.46

[a] ITC titration curve could not be fitted without large errors.

Conclusions

In summary we show in a highly competitive solvent, resorcinarenes prefer fused aromatic N-heterocycles. While quinoline form 1:1 open inclusion complex, the corresponding phenanthroline templates a dimeric capsule in pure methanol. The dimeric capsule was confirmed through 2D DOSY analysis and X-ray crystallography. In a mixed methanol-chloroform mixture (50/50 v/v), both N-heterocycles form 1:1 open inclusion complexes. The addition of a halogen bond donor, 1-iodononafluorobutane, revealed halogen bond formation with the anchored N-heterocycle inside the resorcinarene in a three-component ternary assembly. The reported N-heterocycle mediation of a resorcinarene-XB1 interaction is a clear example of ternary architecture in a highly competitive solvent environment. The formation of the binary and ternary systems is investigated in solution through ^{1}H, ^{13}C, ^{19}F and DOSY NMR analysis as well. The electron-rich resorcinarene cavity makes the pyridine N-atom more basic through the host-guest C–H···π interactions. The ITC-derived thermodynamic parameters (negative ΔH and positive $T\Delta S$ values) for the **Qu**-**XB1** binary system indicate that complexation is enthalpy driven and compensated by entropy, while it is both enthalpically and entropically favored in the case of **MeC2**-**Qu**. The X-ray structure permits direct observation of the weak interactions between the **Phen** and the **MeC2** in pure methanol. The N-heterocycle guest in the cavity of the host can achieve positions for halogen bonding in a very competitive solvent environment which was far less obvious in the binary system.

Experimental Section

General information: The C_{ethyl}-2-methylresorcinarene was synthesized according to reported procedures.[53] The guests, naphthalene, phenanthrene, quinoline, and phenanthroline, and the XB donor 1-iodononafluorobutane, and solvents used for syntheses, NMR and ITC experiments, and crystallizations were purchased from Sigma Aldrich or Oakwood Chemicals (Estill SC, USA). The ^{1}H, ^{13}C, ^{19}F-NMR, and DOSY NMR experiments were carried out in either CD_3OD or $CD_3OD/CDCl_3$ 50/50, v/v at 298 K on either Bruker Avance 300 or 400 MHz spectrometers. **ITC** measurements were performed using VP-ITC instrument made by MicroCal.

Solid-state X-ray crystallography: The data was measured using a dual-source Rigaku SuperNova diffractometer equipped with an Atlas detector and an Oxford Cryostream cooling system using mirror-monochromated Cu-Kα radiation (λ = 1.54184 Å). Data collection and reduction for all complexes were performed using the program CrysAlisPro[54] and Gaussian face-index absorption correction method was applied. The structure is solved with intrinsic phasing (SHELXT)[54] and refined by full-matrix least squares on F^2 using the *OLEX2* software[55], which utilizes the *SHELXL*-2015 module.[56] Non-hydrogen atoms were assigned anisotropic displacement parameters unless stated otherwise. Hydrogen atoms were placed in idealized positions and included as riding. Isotropic displacement parameters for all H atoms were constrained to multiples of the equivalent displacement parameters of their parent atoms either with $U_{iso}(H)$ = 1.2 or 1.5 U_{eq} (parent atom). Several reflections with large discrepancies between the calculated and observed structure factors have been omitted from the least-squares refinement as outliers. Distance restraints (DFIX) and constraints (AFIX) were applied. Positional disorders were refined to two split positions, with the sum of the site occupancies of both alternative positions constrained to either half or unity (see the cif file). The X-ray crystal data and experimental details and CCDC number are given below.

Data for Phen@(MeC2)$_2$: CCDC Number: 2231744. $C_{92}H_{122}N_2O_{25}$, M = 1655.91 g·mol^{-1}, brown block, 0.13 × 0.09 × 0.05 mm^3, triclinic, space group P-1 (No. 2), a = 11.3550(4) Å, b = 11.5120(4) Å, c = 17.7648(6) Å, α = 95.134(3)°, β = 104.049(3)°, γ = 107.726(3)°, V = 2111.97(13) $Å^3$, Z = 1, D_{calc} = 1.302 g·cm^{-3}, F(000) = 888, μ = 0.772 mm^{-1}, T = 123(2) K, θ_{max} = 66.749°, 11973 total reflections, 5587 with Io > 2σ(Io), R_{int} = 0.0416, 7359 data, 610 parameters, 0 restraints, GooF = 1.019, R_1 = 0.0644 and wR_2 = 0.1710 [Io > 2σ(Io)], R_2 = 0.0842 and wR_2 = 0.1860 (all reflections), 0.611 < dΔρ < −0.355 e$Å^{-3}$.

Synthesis of Phen@(MeC2)$_2$: **MeC2** (5 mg 0.0076 mmol, 1 equiv.), **Phen** (1.5 mg, 0.0082 mmol, 1.1 equiv.), and MeOH (1 mL) are added to a 5 mL vial at room temperature. Using a vortex mixer, the components were stirred roughly for 15 seconds. Slow evaporation of the resultant brown solution at ambient temperature gave single crystals suitable for X-ray diffraction analysis after one week.

NMR solution experiments: ^{1}H, ^{13}C, ^{19}F, and DOSY NMR spectra were recorded on a Bruker Avance 300 MHz and 400 MHz spectrometers. All signals are given as δ values in ppm relative to TMS using residual solvent signals as the internal standard. For sample preparation, stock solutions of the receptor **MeC2** (60 mM), the guests (**Qu, Phen, Np**, and **Phe**, 60 mM), and all the XB donor **XB1** (60 mM) were prepared in either CD_3OD or $CD_3OD/CDCl_3$ v/v. For the pure samples, 200 μL of the stock solution was transferred to an NMR tube and diluted with 400 μL of pure solvent providing a 20 mM sample concentration. For a 1:1 mixture, as an example, 200 μL of **MeC2**, 200 μL of **Qu** and 200 μL of pure solvent provided a 20 mM sample concentration of each component in the mixture. For a 1:1:1 mixture, as an example, 200 μL of **MeC2**, 200 μL of **Qu**, and 200 μL of each **XB1** were mixed to give a 20 mM sample concentration of each component in the mixture.

ITC solution experiments: A VP-ITC instrument by MicroCal was used to determine the molar enthalpy (ΔH) of complexation. Subsequent fitting of the data to a 1:1 binding model using Origin software provides association constant (K), change in enthalpy (ΔH) and entropy (ΔS). The ITC experiment was carried out by filling the sample cell with one sample (0.25 mM), filling the syringe with the second sample (5.0 mM), and titrating via computer-automated injector at 298 K. Blank titrations into plain solvent were also performed, and subtracted from the corresponding titration to remove any effect from the heats of dilution from the titrant.

Acknowledgments

We gratefully acknowledge financial support from the American Chemical Society (NKB: ACS-PRF grant no. 39427), Oakland University, MI, the Academy of Finland (KR: grant no. 317259), and the University of Jyväskylä. We also acknowledge the financial support from the Natural Sciences and Engineering Research Council of Canada (JFT: grant no. 2018-06338) and the Ontario Early Researcher Award (JFT: grant no. ER18-14-114).

Keywords: Halogen bond • Resorcinarenes • Ternary assemblies • Dimeric capsules • N-Heterocycles

References

[1] J. R. Moran, S. Karbach, D. J. Cram, *J. Am. Chem. Soc.* **1982**, *104*, 5826–5828.

[2] N. Nishimura, K. Kobayashi, *Angew. Chem. Int. Ed.* **2008**, *47*, 6255–6258.

[3] K. Twum, K. Rissanen, N. K. Beyeh, *Chem. Rec.* **2021**, *21*, 386–395.

[4] K. Twum, A. Bhattacharjee, E. T. Laryea, J. Esposto, G. Omolloh, S. Mortensen, M. Jaradi, N. L. Stock, N. Schileru, B. Elias, E. Pszenica, T. M. McCormick, S. Martic, N. K. Beyeh, *RSC Med. Chem.* **2021**, *12*, 2022–2030.
[5] J. Rebek, *Acc. Chem. Res.* **2009**, *42*, 1660–1668.
[6] T. Evan-Salem, I. Baruch, L. Avram, Y. Cohen, L. C. Palmer, J. Rebek, *Proc. Natl. Acad. Soc. U. S. A.* **2006**, *103*, 12296–12300.
[7] L. Adriaenssens, P. Ballester, *Chem. Soc. Rev.* **2013**, *42*, 3261–3277.
[8] S. M. Taimoory, K. Twum, M. Dashti, F. Pan, M. Lahtinen, K. Rissanen, R. Puttreddy, J. F. Trant, N. K. Beyeh, *J. Org. Chem.* **2020**, *85*, 5884–5894.
[9] Nakayama Tomonari, Nomura Masayoshi, Haga Kohji, Ueda Mitsuru, *Bull. Chem. Soc. Jpn.* **1998**, *71*, 2979–2984.
[10] A. R. Kongor, V. A. Mehta, K. M. Modi, M. K. Panchal, S. A. Dey, U. S. Panchal, V. K. Jain, *Top. Curr. Chem.* **2016**, *374*, 1–46.
[11] L. D. Pedro-Hernández, E. Martínez-Klimova, S. Cortez-Maya, S. Mendoza-Cardozo, T. Ramírez-Ápan, M. Martínez-García, *Nanomaterials* **2017**, *7*, 163.
[12] Y. Matsushita, T. Matsui, *Tetrahedron Lett.* **1993**, *34*, 7433–7436.
[13] K. Mahadevan, V. S. Patthipati, S. Han, R. J. Swanson, E. C. Whelan, C. Osgood, R. Balasubramanian, *Nanotechnology* **2016**, *27*, 335101.
[14] A. Kalgutkar, D. Dalvie, J. O'Donnell, T. Taylor, D. Sahakian, *Curr. Drug. Metab.* **2005**, *3*, 379–424.
[15] V. R. Solomon, H. Lee, *Curr. Med. Chem.* **2011**, *18*, 1488–1508.
[16] F. Hu, L. Zhang, K. S. Nandakumar, K. Cheng, *Curr. Top. Med. Chem.* **2021**, *21*, 2514–2528.
[17] F. Nachon, E. Carletti, C. Ronco, M. Trovaslet, Y. Nicolet, L. Jean, P. Y. Renard, *Biochem. J.* **2013**, *453*, 393–399.
[18] J. S. Carey, D. Laffan, C. Thomson, M. T. Williams, *Org. Biomol. Chem.* **2006**, *4*, 2337–2347.
[19] E. Vitaku, D. T. Smith, J. T. Njardarson, *J. Med. Chem.* **2014**, *57*, 10257–10274.
[20] M. Nissinen, K. Rissanen, *Supramol. Chem.* **2011**, *15*, 581–590.
[21] F. Biedermann, H. J. Schneider, *Chem. Rev.* **2016**, *116*, 5216–5300.
[22] E. O. M. Orlemans, W. Verboom, M. W. Scheltinga, D. N. Reinhoudt, P. Lelieveld, H. H. Fiebig, B. R. Winterhalter, J. A. Double, M. C. Bibby, *J. Med. Chem.* **1989**, *32*, 1612–1620.
[23] R. G. Thorave, D. N. Lande, S. v. Athare, S. P. Gejji, R. G. Gonnade, D. D. Malkhede, *J. Mol. Liq.* **2017**, *246*, 187–196.
[24] S. Bélanger, M. Gilbertson, D. I. Yoon, C. L. Stern, X. Dang, J. T. Hupp, *J. Chem. Soc., Dalton Trans.* **1999**, *0*, 3407–3411.
[25] K. Kobayashi, Y. Asakawa, Y. Kato, Y. Aoyama, *J. Am. Chem. Soc.* **1992**, *114*, 10307–10313.
[26] P. Metrangolo, F. Meyer, T. Pilati, G. Resnati, G. Terraneo, *Angew. Chem. Int. Ed.* **2008**, *47*, 6114–6127.
[27] G. R. Desiraju, P. Shing Ho, L. Kloo, A. C. Legon, R. Marquardt, P. Metrangolo, P. Politzer, G. Resnati, K. Rissanen, *Pure Appl. Chem.* **2013**, *85*, 1711–1713.
[28] T. Clark, M. Hennemann, J. S. Murray, P. Politzer, *J. Mol. Model.* **2007**, *13*, 291–296.
[29] J. Rebek, *Acc. Chem. Res.* **2009**, *42*, 1660–1668.
[30] P. Politzer, P. Lane, M. C. Concha, Y. Ma, J. S. Murray, *J. Mol. Model.* **2007**, *13*, 305–311.
[31] M. G. Sarwar, D. Ajami, G. Theodorakopoulos, I. D. Petsalakis, J. Rebek, *J. Am. Chem. Soc.* **2013**, *135*, 13672–13675.
[32] X. Ma, Y. Zhao, *Chem. Rev.* **2015**, *115*, 7794–7839.
[33] T. Ogoshi, T. A. Yamagishi, Y. Nakamoto, *Chem. Rev.* **2016**, *116*, 7937–8002.
[34] G. Yu, K. Jie, F. Huang, *Chem. Rev.* **2015**, *115*, 7240–7303.
[35] W. Wang, X. Wang, J. Cao, J. Liu, B. Qi, X. Zhou, S. Zhang, D. Gabel, W. M. Nau, K. I. Assaf, H. Zhang, *Chem. Commun.* **2018**, *54*, 2098–2101.
[36] L. K. S. von Krbek, C. A. Schalley, P. Thordarson, *Chem. Soc. Rev.* **2017**, *46*, 2622–2637.
[37] P. Thordarson, *Chem. Soc. Rev.* **2011**, *40*, 1305–1323.
[38] E. L. Kovrigin, *J. Biomol. NMR* **2012**, *53*, 257–270.
[39] D. H. Williams, M. S. Searle, J. P. Mackay, U. Gerhard, R. A. Maplestone, *Proc. Natl. Acad. Soc. U. S. A.* **1993**, *90*, 1172–1178.
[40] A. Shivanyuk, J. Rebek, *J. Am. Chem. Soc.* **2003**, *125*, 3432–3433.
[41] L. Avram, Y. Cohen, *Org. Lett.* **2003**, *5*, 3329–3332.
[42] Q. Zhang, L. Catti, K. Tiefenbacher, *Acc. Chem. Res.* **2018**, *51*, 2107–2114.
[43] M. Chwastek, P. Cmoch, A. Szumna, *J. Am. Chem. Soc.* **2022**, *144*, 5350–5358.
[44] A. Kiesilä, N. K. Beyeh, J. O. Moilanen, R. Puttreddy, S. Götz, K. Rissanen, P. Barran, A. Lützen, E. Kalenius, *Org. Biomol. Chem.* **2019**, *17*, 6980–6984.
[45] D. M. Vriezema, M. C. Aragonès, J. A. A. W. Elemans, J. J. L. M. Cornelissen, A. E. Rowan, R. J. M. Nolte, *Chem. Rev.* **2005**, *105*, 1445–1489.
[46] N. K. Beyeh, R. Puttreddy, K. Rissanen, *RSC Adv.* **2015**, *5*, 30222–30226.
[47] D. P. Weimann, C. A. Schalley, *Supramol. Chem.* **2008**, *20*, 117–128.
[48] H. Mansikkamäki, M. Nissinen, C. A. Schalley, K. Rissanen, *New J. Chem.* **2003**, *27*, 88–97.
[49] N. K. Beyeh, A. Valkonen, K. Rissanen, *Supramol. Chem.* **2010**, *21*, 142–148.
[50] G. v. Oshovsky, D. N. Reinhoudt, W. Verboom, *Angew. Chem. Int. Ed.* **2007**, *46*, 2366–2393.
[51] H. Mansikkamäki, M. Nissinen, C. A. Schalley, K. Rissanen, *New J. Chem.* **2003**, *27*, 88–97.
[52] M. Kolář, J. Hostaš, P. Hobza, *Phys. Chem. Chem. Phys.* **2014**, *16*, 9987–9996.
[53] N. K. Beyeh, D. P. Weimann, L. Kaufmann, C. A. Schalley, K. Rissanen, *Chem. Eur. J.* **2012**, *18*, 5552–5557.
[54] G. M. Sheldrick, *Acta. Cryst. C* **2015**, *71*, 3–8.
[55] O. v. Dolomanov, L. J. Bourhis, R. J. Gildea, J. A. K. Howard, H. Puschmann, *J. Appl. Crystallogr.* **2009**, *42*, 339–341.
[56] G. M. Sheldrick, *Acta. Cryst. A* **2015**, *71*, 3–8.

10.1002/asia.202201308

WILEY-VCH

RESEARCH ARTICLE

Entry for the Table of Contents

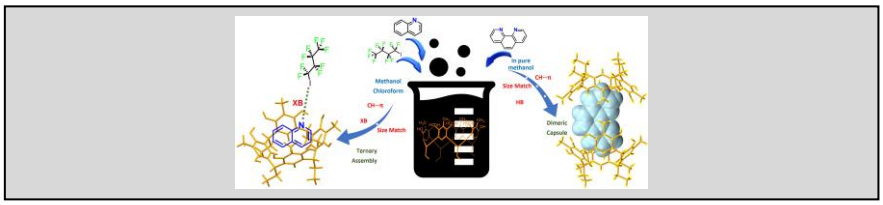

Fused aromatic N-heterocycles quinoline templates a halogen-bonded ternary assembly with resorcinarene and 1-iodonoonafluorobutane in a highly competitive solvent environment, while phenanthroline templates a dimeric capsule in pure methanol.

Institute and/or researcher Twitter usernames: @Beyeh_lab, @oaklandu